STUDY OF PROJECTION MOIRÉ TECHNIQUE APPLIED TO FREE CONTOUR MEASUREMENTS IN BIOENGINEERING

Sara Del-Vecchio
saradvec@yahoo.com.br

Inácio Loiola Pereira Campos
inaciolpcampos@aol.com

Meinhard Sesselmann
meinhard@ufmg.br

Marcos Pinotti
Laboratório de Bioengenharia - Labbio
Departamento de Engenharia Mecânica
Universidade Federal de Minas Gerais UFMG - Avenida Antônio Carlos, 6627, Pampulha, Belo Horizonte – Minas Gerais
CEP: 31270-901
pinotti@ufmg.br

Abstract. *One of the greatest challenges of Bioengineering is the correct diagnostics, without health injury, of pathologies associated with human body deformities. In this work, an optical system of projection Moiré is presented. It is composed of a high resolution LCD projector and a digital photographic CCD camera. The configuration of the optical system is such that the projection unit illuminates the specimen surface at an angle of forty five degrees while the camera observes the specimen under test normally to its surface. A human foot moulded on plaster was used to test the measurement performance of the system. Parallel grating patterns were obtained digitally and projected upon the surface to be measured. Moreover, to quantify these free form contours, a dedicated software was developed. This software calculates the 3D profile from two dimensional grey level images using the phase-shifting technique. The measured foot using projection moiré technique is compared to the measurement data of the same foot got from a coordinate measuring machine (CMM). Moreover, a brief metrological analysis of the possible measurement uncertainties is presented. The main advantadges of the proposed system are its relative easy set up justified by the standard optical components and absense of any moving parts. Measurements results obtained with the proposed system demonstrate its applicability in Bioengineering.*

Keywords*: Projection Moiré, bioengineering, optical system, free contours, 3D profiles, phase shifting*

1. Introduction

In optics the term Moiré refers to a beat pattern produced between two gratings of approximately equal spacing. It can be seen in every day things such as the overlapping of two window screens or with a striped shirt seen on television (Creath, 1993). “Figure 1” shows Moiré pattern produced by two identical straight line gratings rotated by a small angle relative to each other.

Projection Moiré techniques were introduced by Brooks and Helfinger in 1969 for optical gauging and deformation measurement. Some of the first uses of Moiré to measure surface topography were reported by Meadows et al.,Takasaki and Wasowski in 1970. Fringe projection is related to optical triangulation using a single point of light and light sectioning where a single line is projected onto an object and viewed in a different direction to determine the surface contour (Creath, 1993).

Takasaki in 1982 found that Moiré techniques were very suitable for measurements of unstable, soft objects such as the human body and they have been widely used in medical research in the detection and assessment of the condition as scoliosis or curvature of the spine.

However, early works were based on fringe counting for quantification. The basic drawbacks of this kind of fringe analysis are great measurement uncertainties and the ambiguity sign inherent in the Moiré fringes. That means, to solve through contour direction, prior information about the specimen is needed (e.g. convex or concave shape). Both drawbacks may be overcome in a measurement system that combines Projection Moiré with Phase-Shifting. The intention of this work is, therefore, to present an optical system based on Projection Moiré and Phase-Shifting, capable of measuring free form contours automatically.

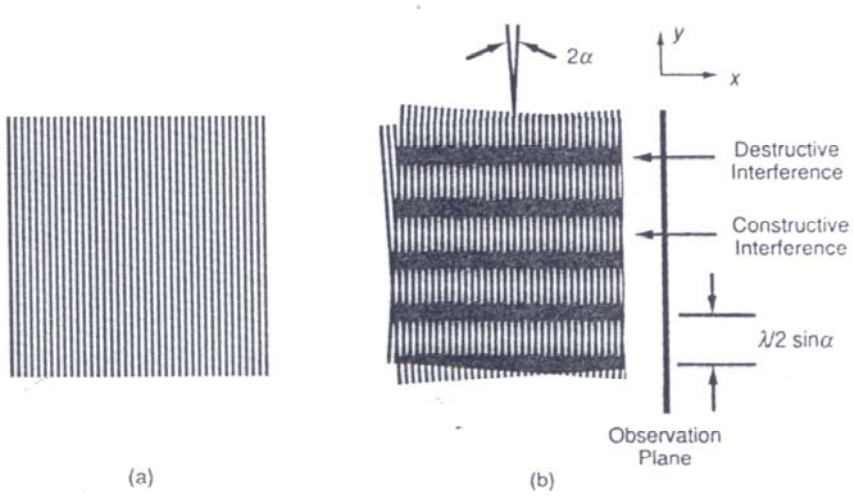

Figure 1 – a- Straight line gratings, b- Moiré between two straight line gratings of the same pitch at an angle α with respect to one another.

2. Methodology

The measurement set-up is shown in "Fig.2". It consists of a LCD projector, with 1024 x 768 pixels resolution, placed at a distance l_p, which projects vertical fringes, i.e. in *y*-direction like shown in "Fig. 1a", under an oblique angle θ upon the specimen surface. A digital CCD camera, with 2048 x 1532pixels resolution, at a distance l_k, observes the fringe pattern normally to the specimen surface, i.e. in *z*-direction. Firstly, the fringe pattern formed by a reference plane (z = 0) is observed. Then, the reference plane is replaced by the free form contour. The resulting fringe pattern is digitally superposed to the previous one producing a beat pattern (Moiré fringes), similar to the process shown in "Fig. 1a". Similarly to Shadow Moiré, it is this Moiré fringe pattern that contains the contour information of the specimen under test. In this work, a human foot moulded on plaster was analysed. The two dimensional digital images (foot plus fringe patterns) were captured by a computer and fed into a specific software in order to retrieve the contour information from the Moiré fringes using the concepts of Projection Moiré.
In order to automatically quantify the surface contour, the measurement technique was combined with Phase-Shifting technique. A phase shift of 360^o was introduced to the grating pattern by lateral translation, such that one fringe exactly replaces its neighbouring fringe. Usually, phase shifting is introduced by lateral displacement of the grating or changing gratings in the form of slides in a slide projector. Here, four digital grating patterns were used for illumination with a LCD projector (beamer). They were digitally displaced in *x*-direction by exactly ¼ of the grating pitch, introducing mutual phase steps of ninety degrees. "Fig. 3" shows the images captured by the CCD camera after each phase step. The bright bars on the specimen surface, detected by the camera, are separated by dark spaces from which much less light is emitted, thus defining fringe visibility. The intensities corresponding to each phase step captured by the camera at *x,y*-pixel position can be expressed by the following equations:

$$I_1 = I_o \cdot [1 + \gamma \cdot \cos\phi] \tag{1}$$

$$I_2 = I_o \cdot [1 + \gamma \cdot \cos\phi + \frac{\pi}{2}] = I_o \cdot [1 - \gamma \cdot \sin\phi] \tag{2}$$

$$I_3 = I_o \cdot [1 + \gamma \cdot \cos\phi + \pi] = I_o \cdot [1 - \gamma \cdot \cos\phi] \tag{3}$$

$$I_4 = I_o \cdot [1 + \gamma \cdot \cos\phi + \frac{3\pi}{2}] = I_o \cdot [1 + \gamma \cdot \sin\phi] \tag{4}$$

Where:
I_i : modulated intensity captured by the CCD camera, for the I^{th} phase step;
I_0 : average intensity ;
γ: detected fringe visibility;
ϕ: phase .

For simplicity the dependency upon *x,y*-pixel position of each variable in "Eq. (1) to (4)" is omitted. Solving the four equations above the phase is given by:

$$\phi = \arctan\left(\frac{I_4 - I_2}{I_1 - I_3}\right) \tag{5}$$

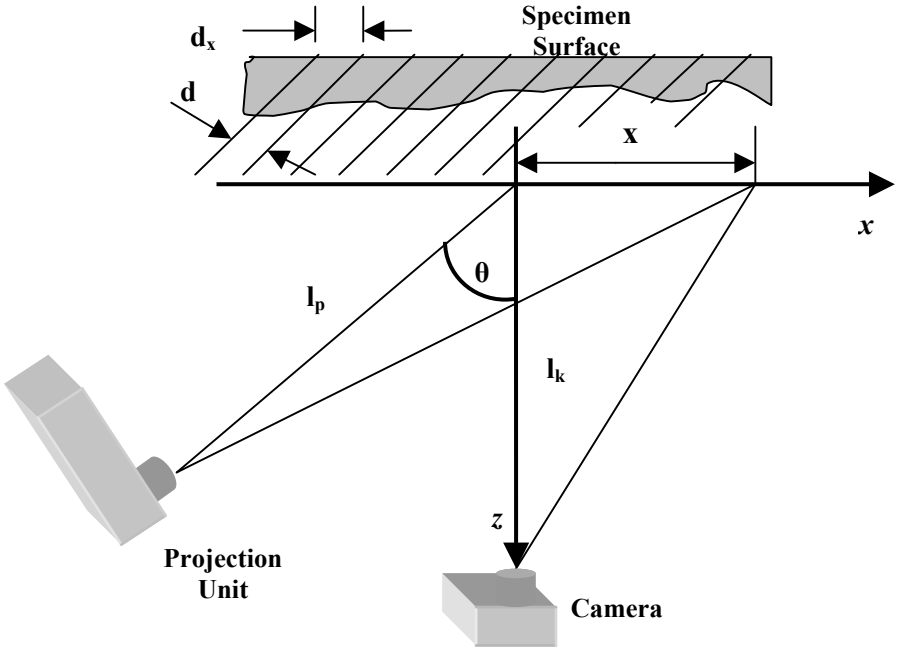

Figure 2: Optical scheme of Projection Moiré.

This phase can be evaluated with an interval of $-\pi \le \phi \le \pi$. The other remaining 2π phase jumps are then removed using phase-unwrapping algorithms. The term phase unwrapping arises because the final step in the fringe pattern measurement process is to unwrap or integrate the phase along a line (or path) counting the 2π discontinuities and adding 2π each time the phase angle jumps from 2π to zero or subtracting 2π if the change is from zero to 2π (Robinson et al., 1993).

After phase unwrapping, two unwrapped phase maps are obtained, one for the reference plane (Ψ_{ref}) and another (Ψ_{obj}) for the studied object surface. The difference between both gives the map of phase difference (Ψ), which is proportional to the surface contour Z, as described by "Eq. (6)":

$$Z = S \cdot lp \cdot \Psi\left[\sin\theta + \frac{(l_k - l_p\cos\theta)\cdot x}{l_k \cdot l_p}\right]^{-1}\left[1 + \frac{x\cdot\sin\theta}{l_p}\right]^2 \tag{6}$$

Where:

Z: Surface depth map;

S: Mounting sensitivity given by the ratio of the grating period with $\theta = 0$ at the specimen surface and its distance to the projection lens;

l_p: Distance between the projection unit and the centre of the studied surface;

l_k: Distance between the digital camera and the centre of the studied surface;

θ: Projection angle;

x: Half object length

ψ: Unwrapped phase difference.

"Equation (6)" shows a significant non-linear dependency of contour Z with increasing *x*. Although the first dependency could be minimised by placing the projector at the same distance from the specimen surface like the camera, the second dependency, however, might not be neglected. This is true because the present system does not obey the condition of Scheimpflug, necessary to keep the projected grating pitch constant and in focus along *x*-direction. For instance, considering a projection angle, θ, of 45°, introducing errors smaller than 1% by neglecting the second dependency on *x*

requires ratios between projector distance and half object length larger than 140. Such large ratios are impossible to achieve with LCD projectors and the second x-dependency in "Eq. (6)" is considered in the calculus of the contour map. According to "Eq. (6)", it is necessary to specify the present optical configuration. In this article, the following geometrical parameter values were considered: l_p of (1,400±10)mm, l_k of (1,000±10)mm, θ of (45±2)° and x of (100±1)mm.

3. Results

The following figures show the studied surface and each shifted fringe pattern used. "Figure 3" shows the analysed plaster human foot and "Fig. 4" shows the reference plane used to apply Moiré, phase shifting and phase unwrapping techniques.

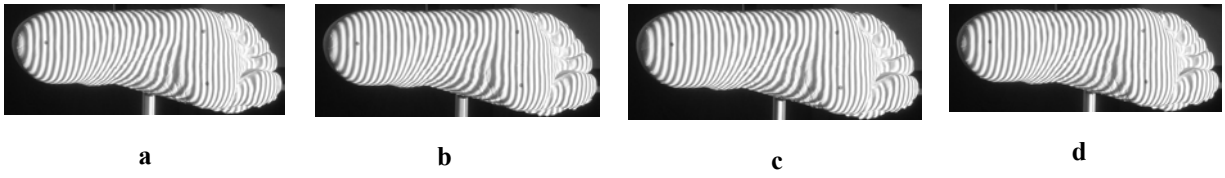

a **b** **c** **d**

Figure 3 – Foot and its four shifted fringes, **a –** 0º; **b** – 90º, **c** – 180º and **d** – 270º.

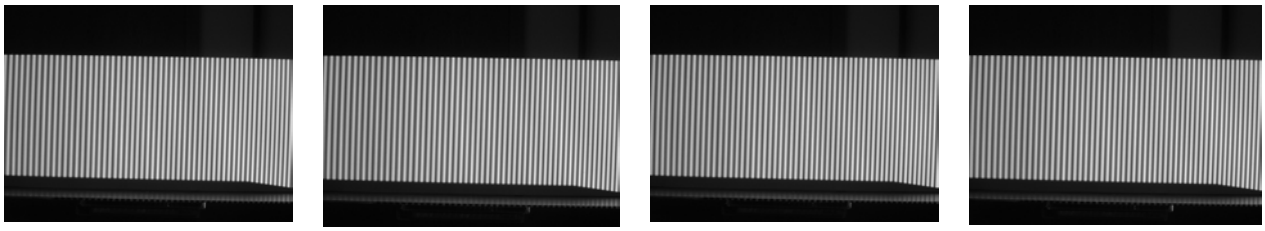

a **b** **c** **d**

Figure 4 – Foot reference plane and its four shifted fringes, **a –** 0º; **b** – 90º, **c** – 180º and **d** – 270º.

Using the concepts of phase shifting and phase unwrapping techniques the processed three dimensional surfaces are presented. The following figures show some of the intermediate results produced by phase shifting and phase unwrapping methods. "Figure 5" illustrates the sine and cosine functions filtered at frequency domain in order to improve data quality. The sine function corresponds to the intensity difference ($I_4 - I_3$) from "Eq. (5)" and, on the same way, the intensity difference ($I_1 - I_2$) represents the cosine function. "Figure 6a" shows the foot phase calculated through sine and cosine functions, according to "Eq. (5)". "Figure 6b" illustrates the pixel area data which delimits the foot contour to be analysed and "Fig. 6c" presents the fringe order map, both of them, interesting data for the phase unwrapping calculation.

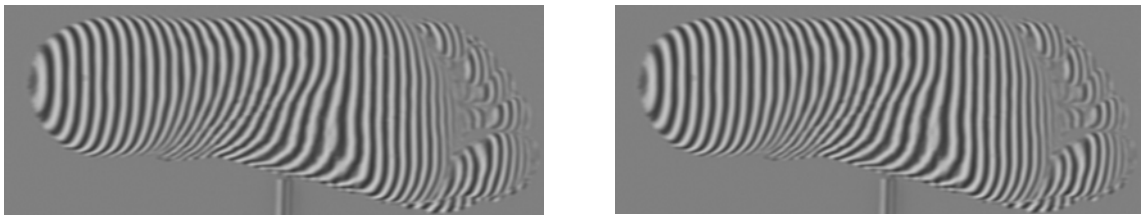

a – Smoothed phase sine **b -** Smoothed phase cosine

Figure 5 - Smoothed phase sine and cosine.

After these calculations, the phase unwrapping was evaluated. The same process calculation procedure was considered for the foot reference. Then, considering the foot and the reference unwrapped phases, the difference of them was calculated. However, as this phase difference map has still kept noise information it was necessary to filter it also at frequency domain. The resultant phase difference is showed at "Fig. 6d".

On a second moment, in order to analyze the Projection Moiré technique measurement performance, a CNC coordinate measurement machine (CMM) was used to get the plaster human foot profile. The CMM described a map file with around 7200 points and a maximum error of ± 0.01mm for each x, y and z directions. Comparing the CMM

uncertainties to the ones expected for Projection Moiré technique, it was reasonable to admit the CMM results as standard parameters. “Figure 7a” shows a two dimensional foot image map got from the CMM and “Fig. 7b” shoes its three dimensional contour. The measured foot obtained by Projection Moiré is represented at “Fig. 7c”, image map, and “Fig. 7d”, shows the three dimensional surface. Both images were produced by 38.875 measurement points collected by the Projection Moiré. To compare the results of both measurement techniques, it was necessary to put them into a common coordinate system. So, calculations were done considering homologous points on the foot surface which were priori known. Working with the same coordinate system it was possible to compute the difference between both images. “Figure 7e” and “Fig. 7f” show the two and three dimensional difference, respectively. Finally, from this difference the measurement error of the Projection Moiré system could be analyzed in comparison to CMM profile. The scale values represented in “Fig. 7” are all in millimeter unit.

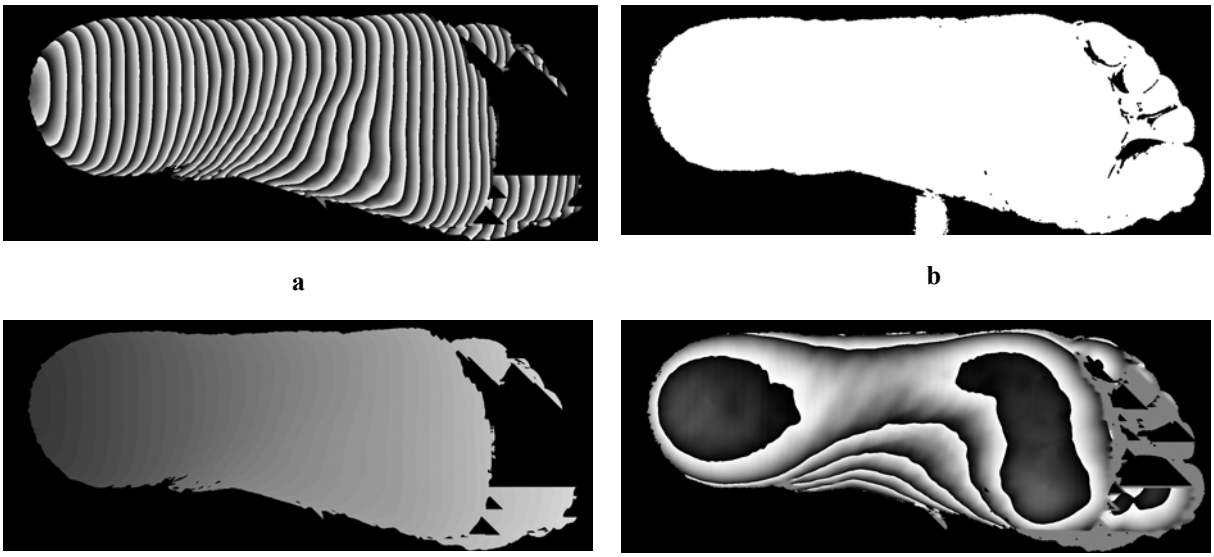

Figure 6 – **a** – Phase map, **b** – Validated pixel area, **c** – Fringe order and **d** – Foot unwrapped phase difference map.

4 Uncertainty analysis

From “Eq. (6)” the following partial differential functions were taken. Rectangular distribution and infinite degrees of freedom were considered to obtain the measurement uncertainties of the projection Moiré methodology.

$$U_{95}^2(Z)=\left(\left|\frac{\partial Z}{\partial S}\right|\cdot U_{95}(S)\right)^2+\left(\left|\frac{\partial Z}{\partial x}\right|\cdot U_{95}(x)\right)^2+\left(\left|\frac{\partial Z}{\partial \psi}\right|\cdot U_{95}(\psi)\right)^2+\left(\left|\frac{\partial Z}{\partial \theta}\right|\cdot U_{95}(\theta)\right)^2+\left(\left|\frac{\partial Z}{\partial l_p}\right|\cdot U_{95}(l_p)+\left|\frac{\partial Z}{\partial l_k}\right|\cdot U_{95}(l_k)\right)^2 \quad (7)$$

$$\frac{U_{95}(Z)}{Z}=\left\{\left(\frac{U_{95}(s)}{s}\right)^2+\left(U_{95}(x)*A\right)^2+\left(\frac{U_{95}(\psi)}{\Psi}\right)^2+\left(U_{95}(\theta)*B\right)^2+\left(\frac{U_{95}(l_p)}{l_p}*C+\frac{U_{95}(l_k)}{l_k}*D\right)^2\right\}^{\frac{1}{2}} \quad (8)$$

Where:

$$A=\left(\frac{l_k-l_p\cdot\cos\theta}{l_p\cdot l_k}\right)\left[\sin\theta+\frac{(l_k-l_p\cdot\cos\theta)\cdot x}{l_p\cdot l_k}\right]^{-1}+\frac{2\sin\theta}{l_p}\left(1+\frac{x\cdot\sin\theta}{l_p}\right)^{-1} \quad (9)$$

$$B=-\left(\cos\theta+\frac{x\cdot\sin\theta}{l_k}\right)\left[\sin\theta+\frac{(l_k-l_p\cos\theta)\cdot x}{l_p l_k}\right]^{-1}+\frac{2x\cdot\sin\theta}{l_p}\left(1+\frac{x\cdot\sin\theta}{l_p}\right)^{-1} \quad (10)$$

$$C=1+\frac{x}{l_p}\cdot\left[\sin\theta+\frac{(l_k-l_p\cos\theta)\cdot x}{l_p\cdot l_k}\right]^{-1}-\frac{2x\cdot\sin\theta}{l_p}\cdot\left(1+\frac{x\cdot\sin\theta}{l_p}\right)^{-1} \quad (11)$$

$$D = \frac{1}{l_k}\left[x \cdot \cot\theta + l_p \cdot \cos\theta - l_k\right] \tag{12}$$

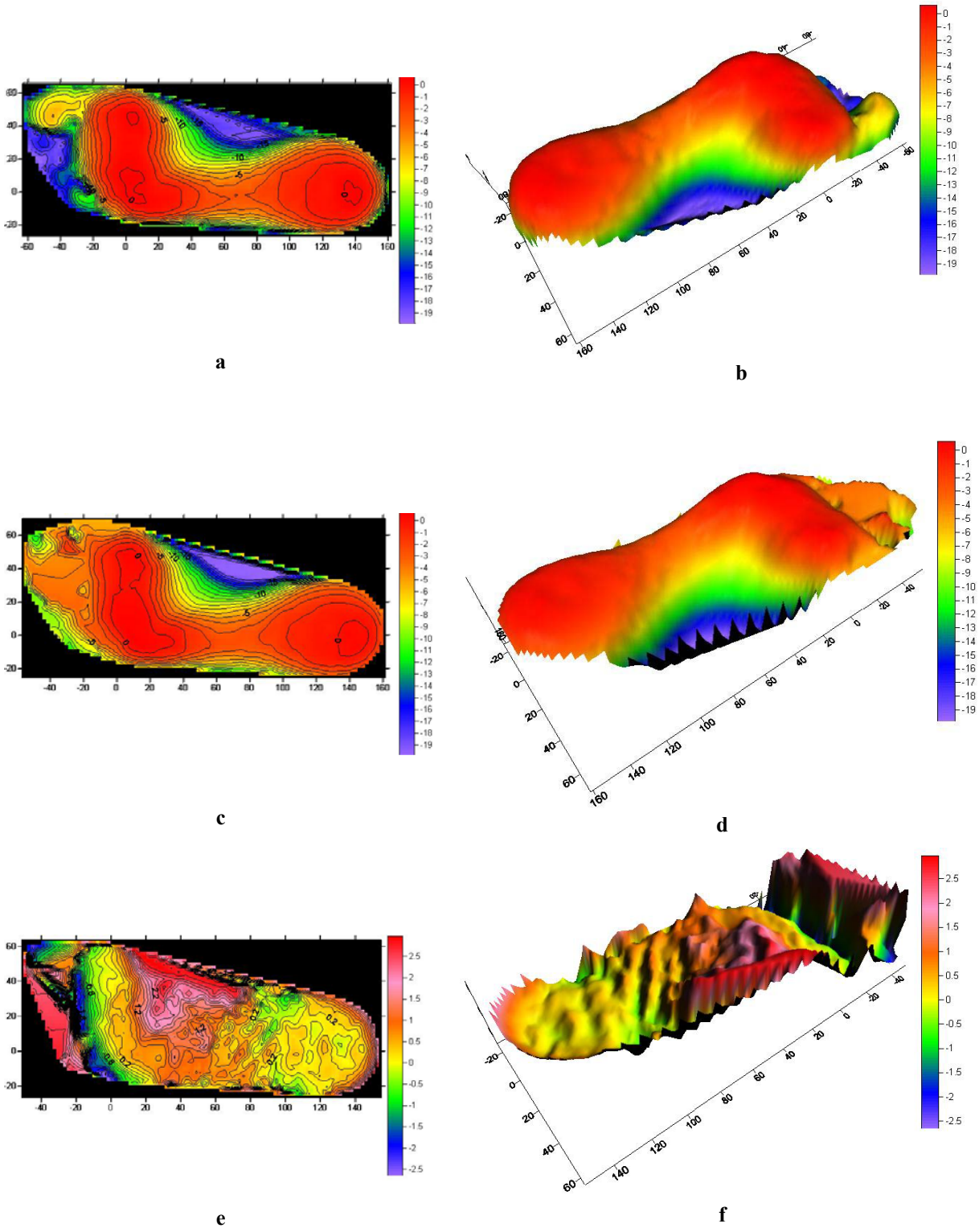

Figure 7 – Comparison of Projection Moiré and CMM foot measurements.

From each parameters considered the following values were adopted: relative expanded uncertainty of S ($U_{95}(s/s)$) equal to 0.01mm, expended uncertainty of x ($U_{95}(x)$) of 1mm, relative expanded uncertainty of ψ ($U_{95}(\psi)/\psi$) of 0.05mm, expended uncertainty of Y ($U_{95}(Y)$) of 0.035mm, relative expanded uncertainty of l_p ($U_{95}(l_p/l_p)$) equal to 0.01mm and relative expanded uncertainty of l_k ($U_{95}(l_k/l_k)$) also equal to 0.01mm.
Taking "Eq. (8)" into consideration and the parameter values listed on the methodology item and also the ones listed above a relative expanded uncertainty value of 6.28% was found. It could be noted that the most relevant uncertainty contributions are the phase uncertainty and the projection angle. This demonstrates that the measurement uncertainty depends greatly from how better phase measurements are processed and also from geometrical system configuration. This uncertainty value can be taking as true mainly if it is compared to the difference error induced by the CMM measurement. However, put both measurement data at the same coordinate system is kind critical and could induce bigger error values than the ones that really exists.

5 Conclusion

The uncertainty analysis presents an error of the same order compared to Shadow Moiré technique. However, software implementation has been still in process to improve the final results. Also the fingers region had a bad resolution which can be justified by the shadows produced during the picture taking phase and also because this region has a critical geometry, full of concavities. On the other hand, it could be seen that the greatest advantage of projection Moiré technique is the simplicity, absence of moving parts and low cost. Moreover, the object length is not a prohibited factor. The studied object can be placed in any position, i.e., vertical or horizontal. Furthermore, it is a non-contact measurement technique, which creates a good advantage for industrial quality control, for example. Another positive characteristic of this optical method is the fact that the data acquisition time is too short compared to CMM.
Furthermore, it is a non-invasive technique that permits human body deformities detection without health injury. So, this method is much appropriated to identify foot and hand deformities and also scoliosis. In addition, this technique can be extended to improve the results of esthetical medicine.

6. Acknowledgements

The authors would like to acknowledge the financial support from CNPq and CAPES and also Dr. Juan Campos Rúbio for making the CMM measurements possible.

7 References

Gasvik, K., J.,1995, "Optical Metrology", Ed. John Wiley & Sons Ltd, New York, USA, 321 p.
Creath, K. 1993, "Interferogram Analysis: Digital fringe pattern measurements technique", avaiable at chapter 4, Ed. David W. Robinson & Graeme T. Reid, 302 p.
Post, D., Han, B. and Ifju, P., 1994, "High sensitivity Moiré: Experimental analysis for mechanics and material", Ed. Springer Verlag, 444 p.
Robinson D. W. and Reid G. T., 1993, "Interferogram Analysis: Digital fringe pattern measurements technique", avaiable at chapter 4, Ed. David W. Robinson & Graeme T. Reid, 302 p.
Su, F.; Yi, S.; Chian, K. S., 2004, "A simple method to unwrap the geometrically discontinuous phase map and its application in the measurement of IC package", Optics and Laser in Engineering, v. 41, n. 2, p. 463-473.
Verleysen, P.; Degriek J., 2004, "A modified digital phase-shift moiré technique for impact deformation measurements", Optics and Laser in Engineering, v. 42, n. 6, p. 623-671, Dez. 2004.
Xie, H.; Shang, H.; Dai, F. Li, B.; Xing, Y., 2004, "Phase shifting SEM moiré method", Optics & Laser Technology, v. 36, n. 4, p. 291-297.

8. Responsibility notice

The authors are the only responsible for the printed material included in this paper.